

URF13, a maize mitochondrial pore-forming protein, is oligomeric and has a mixed orientation in *Escherichia coli* plasma membranes

(membrane protein topology/protein cross-linking/cytoplasmic male sterility/*Bipolaris maydis* race T)

KENNETH L. KORTH*, CYRIL I. KASPI†, JAMES N. SIEDOW†, AND CHARLES S. LEVINGS III*‡

*Department of Genetics, North Carolina State University, Raleigh, NC 27695-7614; and †Department of Botany, Duke University, Durham, NC 27706

Contributed by Charles S. Levings III, August 28, 1991

ABSTRACT URF13, an inner mitochondrial membrane protein of the maize Texas male-sterile cytoplasm (*cms-T*), has one orientation in the inner membrane of maize mitochondria but two topological orientations in the plasma membrane when expressed in *Escherichia coli*. Antibodies specific for the carboxyl terminus of URF13 and for an amino-terminal tag fused to URF13 in *E. coli* were used to determine the location of each end of the protein following protease treatments of right-side-out and inside-out vesicles derived from *cms-T* mitochondria and the *E. coli* plasma membrane. Cross-linking studies indicate that a portion of the URF13 population in mitochondria and *E. coli* exists in membranes in an oligomeric state and, in combination with proteolysis studies, show that individual subunits within a given multimer have the same orientation. A three-membrane-spanning helical model for URF13 topology is presented.

URF13 is a mitochondrially encoded 13-kDa protein uniquely associated with the inner mitochondrial membrane of maize carrying the Texas male-sterile cytoplasm (*cms-T*) (1–3). The DNA encoding URF13 (*T-urf13*) arose by multiple recombinational events and contains nucleotide sequences derived from four disparate origins (4). The open reading frame is made up of sequences originating from coding and flanking regions of the mitochondrial 26S rRNA gene and a small region of unknown origin. *cms-T* maize fails to produce viable pollen and is particularly susceptible to two fungal pathogens, *Bipolaris maydis* race T and *Phyllosticta maydis*. These pathogens caused widespread disease in the United States maize crop in 1969 and 1970 and effectively stopped the use of *cms-T* maize for the production of hybrid seed. Maize carrying normal cytoplasm is not seriously affected by these pathogens (reviewed in ref. 5). Isolated *cms-T* maize mitochondria exposed to specific toxins (T toxins) produced by these fungal pathogens exhibit swelling, inhibition of malate-stimulated respiration, uncoupling of oxidative phosphorylation, and leakage of small molecules and ions (NAD⁺ and Ca²⁺). Identical effects are seen when *cms-T* mitochondria are exposed to methomyl, an insecticide structurally unrelated to T toxins (reviewed in ref. 6). The T toxin/URF13 interaction results in pore formation in the *cms-T* inner mitochondrial membrane (5).

Escherichia coli expressing the cloned *T-urf13* gene product respond to T toxin or methomyl like *cms-T* mitochondria (7, 8). This observation provides direct evidence that URF13 is responsible for susceptibility of *cms-T* maize to the fungal toxins. The analogous responses of *cms-T* maize mitochondria and *E. coli* to T toxins or methomyl suggest that URF13 has comparable structural and topographical properties in both membrane systems.

P. maydis toxin has been shown to cooperatively bind to URF13 produced in *E. coli*. The binding is reversible, and T toxins and methomyl compete for the same or overlapping binding sites (9). A possible explanation for the cooperative binding is that URF13 exists in the membrane as a multimeric complex and that binding of toxin to one URF13 subunit facilitates subsequent toxin binding to other subunits within the complex. To address the oligomeric nature of URF13, cross-linking studies were carried out with *cms-T* mitochondria and *E. coli* expressing URF13. The results suggest that a portion of the URF13 population exists in the membrane as oligomeric units.

We have used protease accessibility studies with *E. coli* spheroplasts and inside-out vesicles (ISOs) to determine the membrane topology of an URF13 fusion product having a short antigenic tag at the amino terminus of the protein. URF13 is in a mixed orientation in the *E. coli* plasma membrane, and the amino and carboxyl termini are located on opposite sides of the membrane, consistent with a postulated three-membrane-spanning helical model (10). *cms-T* maize mitoplasts and submitochondrial particles (SMPs) were used to examine the membrane topology of URF13 in mitochondria. The carboxyl terminus is located on the matrix side of the inner mitochondrial membrane.

MATERIALS AND METHODS

Construction of pET5.13T. DNA cleavage, ligation, and introduction of plasmid DNA into *E. coli* were done as described (11). A 2013-base-pair (bp) *Hind*III fragment from the *cms-T* mitochondrial genome (4) was ligated into pBlue-scriptII KS⁺ (Stratagene). A *Bam*HI restriction site was created six nucleotides upstream of the first base of the *T-urf13* open reading frame via site-directed mutagenesis (12). A 511-bp *Bam*HI/*Bgl* II fragment containing the entire *T-urf13* open reading frame was ligated into pET5b (Novagen, Madison, WI) (13) to create pET5.13T. The amino terminus of the fusion peptide encoded by pET5.13T (s10:URF13) has the sequence H₂N-Met-Ala-Ser-Met-Thr-Gly-Gly-Glu-Glu-Met-Gly-Arg-Asp-Pro-Met- . . . (where Met represents the initial methionine residue of the wild-type URF13 protein). The first 11 residues of the fusion protein are identical to a portion of the ϕ T7 gene 10 protein (s10). Antiserum specific for s10 was obtained from Novagen.

Antibody Production and Screening. URF13 was expressed with the pLC13T construct in *E. coli* as described (8). URF13 was purified from *E. coli* extracts by 18% SDS/PAGE, electroeluted, and injected into BALB/c mice. Immunogen preparation and antibody screening were done as described (14), and monoclonal antibodies (MAbs) were prepared according to ref. 15.

The publication costs of this article were defrayed in part by page charge payment. This article must therefore be hereby marked "advertisement" in accordance with 18 U.S.C. §1734 solely to indicate this fact.

Abbreviations: SMP, submitochondrial particle; ISO, inside-out *E. coli* vesicle; EGS, ethylene glycolbis(succinimidylsuccinate); DST, disuccinimidyl tartrate; MAb, monoclonal antibody.

‡To whom reprint requests should be addressed.

s10:URF13 Induction and Preparation of ISOs and Spheroplasts. Production of s10:URF13 in *E. coli* strain BL21(DE3) pLysS was induced as recommended by Novagen. The sensitivity of cell respiration to methomyl and T toxin was measured with a Clark O₂ electrode (7). *E. coli* spheroplasts were prepared as described (16). ISOs were formed by passing spheroplasts through a French pressure cell at 7500 psi (1 psi = 6.89 kPa) (17) and isolated on sucrose gradients (18). For proteolysis and cross-linking experiments, spheroplasts and ISOs were diluted to 1 mg/ml of protein in 0.25 M sucrose and 0.1 M Tris (pH 8.0) or 20 mM KHPO₄ (pH 7.4), respectively.

Mitochondrial Preparations. Washed *cms-T* maize mitochondria were isolated from 6-day-old etiolated seedlings as described (19). Mitoplasts were formed by resuspension of washed mitochondrial pellets in 0.7 M mannitol/0.1% bovine serum albumin/1.0 mM MgCl₂/20 mM Hepes, pH 7.2, followed by passage through a French pressure cell at 3000 psi (20). The preparation was diluted 4-fold with wash buffer (0.4 M mannitol/0.1% bovine serum albumin/0.1 mM EDTA/20 mM Hepes, pH 7.2) and centrifuged at 12,000 × *g* for 10 min. The resulting mitoplast pellet was resuspended in wash buffer at 1.0 mg/ml of protein for all experiments. The ratio of mitoplasts to intact mitochondria was determined by a cytochrome *c* oxidase assay (21). SMPs, oriented with the matrix side exposed, were generated by sonication of washed mitochondria (22).

Proteolysis. Final working protease concentrations were 0.01 mg of trypsin per ml (Sigma type XIII) and 0.1 mg of proteinase K per ml (Boehringer Mannheim). Protease treatments were performed at 22°C in the absence and presence of permeabilizing levels of Triton X-100. Proteolysis was terminated with SDS/PAGE loading buffer containing 8 mM phenylmethylsulfonyl fluoride and boiling the samples for 5 min. Samples were separated by 18% SDS/PAGE as described (8) without urea. Immunoblotting was carried out as described (14).

Cross-Linking. Cross-linking of URF13 was carried out with the lysine-specific, hydrophobic reagents ethylene glycolbis(succinimidylsuccinate) (EGS) and disuccinimidyl tartrate (DST) (Pierce). Cross-linking reagent (5 mM) was incubated at room temperature with either isolated *cms-T* mitochondria or whole *E. coli* cells (in 50 mM potassium phosphate buffer, pH 7.0) at 1 mg/ml of protein. After 5 min of incubation, the reaction was quenched by the addition of 40 mM glycine.

RESULTS

Cross-Linking. *E. coli* cells expressing wild-type URF13 (pLC13-T) cross-linked with either EGS, a 16.1-Å reagent, or DST, a 6.4-Å reagent, repeatedly showed a band at 25 kDa, consistent with formation of an URF13 dimer (Fig. 1, lanes 2 and 3). Reaction with EGS also gave rise to a weaker band that had mobilities on SDS/PAGE expected of a trimeric species (Fig. 1, lane 3). No such bands appeared when no cross-linking reagent was added to *E. coli* cells expressing URF13 (Fig. 1, lane 1). Time-course experiments showed an accumulation of the higher molecular mass species with increased reaction time, but neither extended incubation times nor higher concentrations of cross-linker eliminated the appearance of monomeric URF13. Mitochondria treated with cross-linkers gave rise to monomeric and dimeric species of URF13 (Fig. 1, lane 5). Cross-linking in the presence of T toxin or methomyl did not alter the observed pattern (Fig. 1, lane 4).

Termini-Specific Markers. Localization of the amino and carboxyl termini of URF13 required antibodies that recognize each end of the molecule. MAbs were raised that recognize either a region of URF13 within the carboxyl-

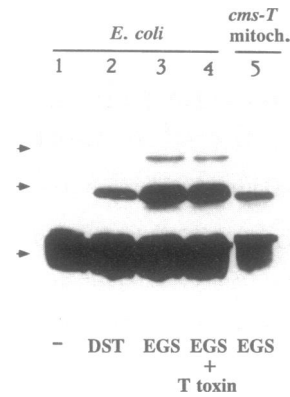


FIG. 1. SDS/PAGE immunoblot of cross-linked *cms-T* mitochondria and *E. coli* expressing URF13. *E. coli* expressing URF13 or isolated *cms-T* mitochondria were incubated for 5 min at room temperature in the absence (lane 1) or presence of either 5 mM DST (lane 2) or EGS (lanes 3–5); the resulting blots were probed with the carboxyl-specific MAb-C. In lane 4, samples were preincubated for 5 min with 10 μ M T toxin. Arrows show location of mono-, di-, and trimeric species.

terminal 14 amino acid residues (MAb-C), as demonstrated by its failure to cross-react with a shortened version of URF13 encoding the amino-terminal 101 residues (full length = 115 residues, data not shown), or an undefined internal portion of the URF13 primary sequence (MAb-I).

Attempts to develop antiserum specific for the amino terminus of URF13 have failed. Therefore, a chimeric gene was constructed, encoding a known epitope at the amino terminus of the full-length URF13 molecule. The pET5b vector (Novagen) was used to fuse 14 amino acid residues, including a sequence from the ϕ T7 s10 protein, to URF13. Cells expressing this fusion product exhibit responses to methomyl and T toxin identical to those seen in *E. coli* expressing wild-type URF13 (data not shown).

Localization of URF13 Termini in *E. coli*. Spheroplasts, in which the periplasmic surface of the *E. coli* plasma membrane is exposed by removal of the outer membrane and cell wall, were prepared from cells expressing the s10:URF13 fusion protein, treated with 0.01 mg of trypsin per ml in the presence or absence of 0.02% Triton X-100, and immunoblotted with antibodies against the s10:URF13 carboxyl and amino termini.

The carboxyl end of some, but not all, of the s10:URF13 molecules is shown to be accessible to trypsin by the significant reduction in signal (Fig. 2A, lane 2) as compared to the uncleaved control (Fig. 2A, lane 1) when MAb-C is used as a probe. Gel migration of the protein product retaining the

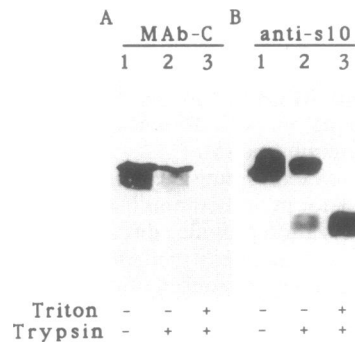


FIG. 2. SDS/PAGE immunoblots of *E. coli* spheroplasts expressing s10:URF13 probed with the carboxyl-specific MAb-C (A) and the amino-specific anti-s10 (B) antibodies. Samples were untreated (lanes 1) or treated with 0.01 mg of trypsin per ml for 20 min without (lanes 2) or with (lanes 3) 0.02% Triton X-100.

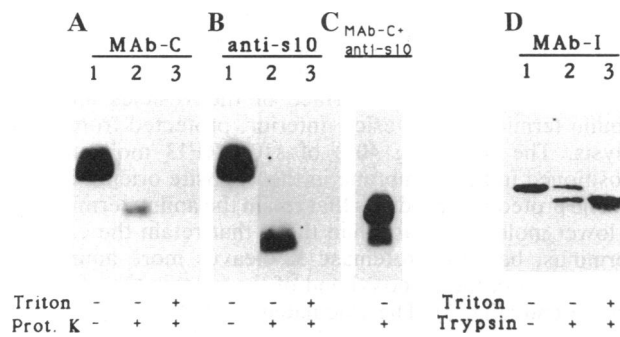


FIG. 3. SDS/PAGE immunoblots of ISOs made from *E. coli* expressing s10:URF13. Blots were probed with the carboxyl-specific MAb-C (A), the amino-specific anti-s10 (B), MAb-C and anti-s10 (C), or MAb-I, an antibody that recognizes an internal region of URF13 (D). Samples were untreated (A, B, and D, lanes 1) or treated for 20 min with either 0.1 mg of proteinase K per ml (A, B, and C) or 0.01 mg of trypsin per ml (D) in the absence (C and A, B, and D, lanes 2) or presence (A, B, and D, lanes 3) of 0.05% Triton X-100.

carboxyl terminus is not changed, suggesting that the amino terminus of s10:URF13 is resistant to trypsin treatment. The intensity of the band reacting with MAb-C is reduced by about 40%, as estimated by densitometry. When Triton X-100 is included in the reaction mixture, making both sides of the membrane accessible, the carboxyl terminus of all of the s10:URF13 is degraded (Fig. 2A, lane 3). Probing these same samples with anti-s10 antiserum confirms that the amino terminus is resistant to trypsin cleavage because the total amount of signal is not significantly reduced by protease treatment. The reduction in size of the protein reacting with the amino-specific antibody results from proteolysis at the carboxyl terminus (Fig. 2B, lanes 2 and 3). Fig. 2A confirms that the carboxyl terminus of only some s10:URF13 molecules is accessible to trypsin in intact spheroplasts (lane 2) but that all carboxyl termini are cleaved in Triton X-100-permeabilized spheroplasts (lane 3). Results similar to those shown in Fig. 2A were obtained when comparable protease treatments were carried out on spheroplasts expressing wild-type URF13 (data not shown), indicating that URF13 topology in the membrane was not affected by the s10:URF13 fusion. Untreated spheroplasts and those exposed to proteinase K for 20 min are equally subject to swelling upon addition of methomyl (data not shown), indicating that protease treatment does not affect URF13 function or compromise the integrity of the *E. coli* plasma membrane.

If *E. coli* plasma membranes are broken into small fragments, they form vesicles that preferentially close in an inside-out manner exposing the cytoplasmic surface (23). When ISOs from cells expressing s10:URF13 are treated with proteinase K, two distinct bands appear on immunoblots, a higher molecular mass band that reacts only with MAb-C

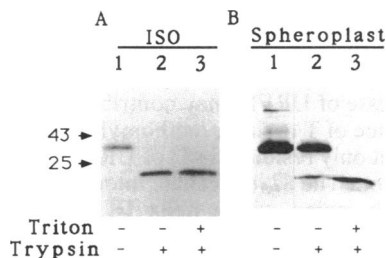


FIG. 4. SDS/PAGE immunoblots of *E. coli* (A) ISOs or (B) spheroplasts probed with anti-SecY antiserum. Samples were untreated (lanes 1) or treated with 0.01 mg of trypsin per ml without (lanes 2) or with (lanes 3) 0.02% Triton X-100. Positions of two molecular mass markers (in kDa) are shown.

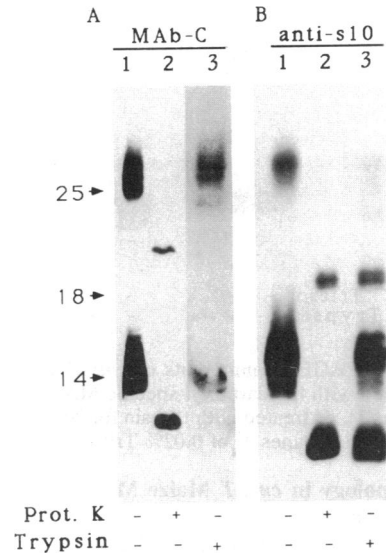


FIG. 5. SDS/PAGE immunoblots of *E. coli* ISOs expressing s10:URF13 that were cross-linked followed by treatment with proteases. Blots were probed with the carboxyl-specific MAb-C (A) or the amino-specific anti-s10 (B). EGS cross-linked ISOs were untreated (lanes 1), treated with proteinase K for 20 min (lanes 2), or treated with trypsin for 20 min (lanes 3). Positions of molecular mass markers (in kDa) are shown.

(Fig. 3A, lane 2) and a lower molecular mass band that reacts only with the anti-s10 antibody (Fig. 3B, lane 2). The species that reacts with MAb-C is 1.5 kDa smaller than the full-length s10:URF13, and the species that reacts with anti-s10 is reduced by 3.6 kDa. Both bands are reduced in intensity relative to the uncleaved control. Probing the same blot with anti-s10 and MAb-C clearly indicates that the two bands represent distinct species (Fig. 3C), each retaining either the amino or carboxyl terminus, but not both. Immunoblotting with MAb-I, an antibody that reacts with an URF13 internal sequence, demonstrates that trypsin treatment of ISOs gives rise to a single shortened version of s10:URF13 in addition to a fraction that remains uncleaved (Fig. 3D).

The fact that both ends of the s10:URF13 molecule show some sensitivity to proteolysis, regardless of vesicle type, suggests that the protein is positioned in the membrane in two orientations. However, these same results would be expected if the protease experiments were carried out using vesicles that are mixed in their orientation. As an independent verification of the orientation of our ISOs and spheroplasts, we took advantage of the well-established sensitivity of the *E. coli* plasma membrane protein SecY to trypsin cleavage on its cytoplasmic surface and its complete insensitivity to trypsin proteolysis on its periplasmic surface (24). Results from immunoblots probed with anti-SecY antiserum show that our ISO preparations are homogeneous, as indicated by the complete absence of full-length SecY in trypsin-treated vesicles (Fig. 4A, lane 2). Scanning densitometry showed $\approx 15\%$ trypsin cleavage of the mature SecY protein in spheroplasts (Fig. 4B, lane 2), indicating that a portion of the cytoplasmic surface was accessible to protease in these preparations.

Cross-Linking Followed by Proteolysis. Proteinase K treatment of EGS cross-linked ISOs expressing s10:URF13 gave rise to two shortened versions of the putative dimeric species of the fusion protein: one that reacted only with MAb-C (Fig. 5A, lane 2) and a second, lower molecular mass species that reacted only with the anti-s10 antibody (Fig. 5B, lane 2). No cross-linked band appeared on these gels that reacted with both antibodies following proteolysis, and no shortened multimeric species were observed that react with MAb-C after trypsin treatment (Fig. 5A, lane 3).

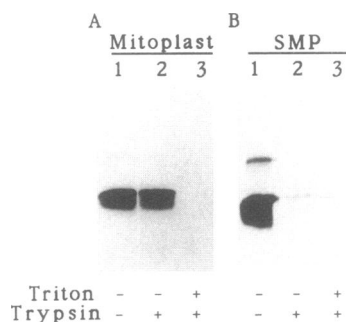


FIG. 6. SDS/PAGE immunoblots of *cms-T* mitoplasts (A) and SMPs (B) probed with the carboxyl-specific MAb-C. Samples were untreated (lanes 1), or treated with trypsin for 20 min in the absence (lanes 2) or presence (lanes 3) of 0.02% Triton X-100.

URF13 Topology in *cms-T* Maize Mitochondria. In *cms-T* maize mitochondria only the protease accessibility of the carboxyl terminus of URF13 could be measured. Mitoplasts were prepared from *cms-T* mitochondria to expose the outer surface of the inner mitochondrial membrane. The level of intact mitoplasts in these preparations was 70–80%, as determined by measuring the accessibility of cytochrome *c* to the inner membrane (21). SMPs were also prepared from *cms-T* mitochondria. The level of inside-out vesicles was 80%, measured with a cytochrome *c* oxidase latency assay (21).

Mitoplasts and SMPs were treated with trypsin and immunoblotted with MAb-C to determine the fate of the carboxyl terminus of URF13. In intact mitoplasts the carboxyl region is largely protected from proteolysis (Fig. 6A, lane 2), whereas addition of 0.02% Triton X-100 results in the complete loss of signal with MAb-C (Fig. 6A, lane 3). In SMPs almost all of the carboxyl terminus of URF13 is digested by trypsin (Fig. 6B, lane 2), suggesting that the carboxyl terminus is localized on the matrix side of the inner mitochondrial membrane.

DISCUSSION

The existence of URF13 oligomers has been postulated based on the cooperative binding of T toxin (9) and the occasional appearance of a dimeric species in SDS/PAGE (Fig. 6) (3). Treatment of *cms-T* mitochondria or *E. coli* with hydrophobic bifunctional cross-linking reagents has revealed an association of URF13 monomers in the membrane. Aggregates of cross-linked URF13 migrate on SDS/PAGE as predicted for dimers and higher order oligomers. Intermediate-size aggregates containing URF13 are not observed, suggesting that URF13 is not closely associated with other proteins to a large extent. The formation of a membrane pore equivalent in size to that formed by URF13 probably requires five or six membrane-spanning α -helices (25). A 115-amino acid residue protein is probably not able to cross a membrane five or six times, and, therefore, URF13 must associate with itself or some other protein(s) to form a pore. Because URF13 can confer pathotoxin sensitivity in several different membrane systems (7, 26, 27), interaction with another specific protein is probably not a requirement for URF13 pore formation in the presence of T toxin.

Two proteolysis products of s10:URF13 remain after proteinase K treatment of ISOs; one retains the carboxyl terminus but lacks the amino terminus, the other lacks the carboxyl terminus while preserving the amino end. Because one end is always protected from proteolysis and the other is cleaved, the s10:URF13 fusion product must cross the membrane an odd number of times. Furthermore, because each end of the protein is partially accessible to protease in closed

vesicles, the s10:URF13 protein must exist in the *E. coli* plasma membrane in two orientations. In ISOs, $\approx 60\%$ of the s10:URF13 molecules have their carboxyl termini located on the outer (cytoplasmic) surface of the vesicles and their amino termini at the vesicle interior, protected from proteolysis. The remaining 40% of s10:URF13 molecules are positioned in the opposite orientation.

The proteolytic products that retain the amino termini have a lower molecular mass than those that retain the carboxyl terminus, because proteinase K cleaves more amino acid residues from the carboxyl end of the protein than from the amino end (Fig. 3). The calculated 3.6-kDa reduction after proteolysis of the carboxyl end corresponds approximately to the removal of amino acid residues 83–115 from the wild-type URF13 protein. These results, which indicate the carboxyl terminus is not protected by the hydrophobic core of the membrane, are consistent with the hydrophilic nature of residues 83–115 (1).

Cross-linking of URF13 in *E. coli* spheroplasts followed by proteinase K treatment demonstrates that in the s10:URF13 dimer, the respective amino and carboxyl termini of each associated subunit are on the same side of the membrane. Dimers made up of subunits having different orientations in the membrane would give rise to proteolysis products reacting with anti-s10 and MAb-C; no such products are observed. The amino terminus of s10:URF13 is resistant to trypsin cleavage. If dimers of mixed orientation were present, then truncated dimers lacking the carboxyl terminus of one subunit but retaining it in the other subunit would be expected after trypsin treatment. No shortened dimeric species that react with MAb-C have been observed after exposure to trypsin (Fig. 5A, lane 3).

In *cms-T* mitochondria the carboxyl terminus of URF13 is located on the matrix side of the inner mitochondrial membrane. This conclusion is based upon the almost complete degradation of the carboxyl terminus when SMPs are exposed to protease, coupled with its remaining largely intact in protease-treated mitoplasts. URF13, like most naturally occurring membrane proteins, thus has one defined orientation in the mitochondrial membrane. This is in marked contrast to the situation in *E. coli* where URF13 exists in two topological orientations. Although no direct proof is available, it is likely that URF13 crosses the inner mitochondrial membrane an odd number of times by analogy with the findings in *E. coli*.

Fig. 7 presents a model of how monomeric URF13 might be positioned in the membrane. Hydrophobicity plots indicate that the carboxyl-terminal region (residues 83–115) is hydrophilic and would not be found within the membrane, which is supported by our proteolysis studies. Residues 13–31 are hydrophobic, making that region a likely candidate for a membrane-spanning domain. Based on calculations of the hydrophobic moment (28), residues 35–55 and 61–83 are predicted to form two amphipathic α -helices (II and III), each having a hydrophobic and hydrophilic face. Consistent with this model, the aspartate residues at positions 12 and 39 are known to covalently bind dicyclohexylcarbodiimide (8), indicating that they are both located in a hydrophobic environment (29). The predicted amphipathic helices in a multimeric aggregate of URF13 may contribute to pore formation in the presence of T toxin or methomyl. Finally, Braun *et al.* (8) found that only residues 1–83 of URF13 are necessary for pore formation. The 82/83 residue interface is situated in the model at the region where helix III interaction with the hydrophobic core of the membrane is predicted to end.

The proposed model contains one interhelical loop connecting the adjacent membrane-spanning regions on each side of the membrane (Fig. 7). We have never observed low molecular mass fragments corresponding to proteolytic cleavage within these areas. The model predicts that these turns are very short, and, therefore, they may not be readily

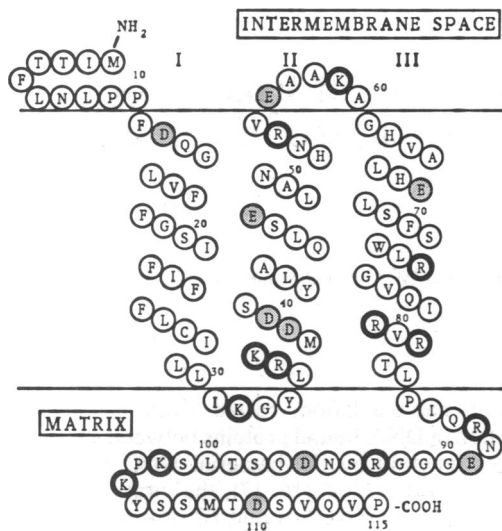


FIG. 7. Proposed membrane topology of an URF13 monomer, with the observed orientation in *cms-T* mitochondria indicated by the MATRIX and INTERMEMBRANE SPACE labels. The three putative α -helices are labelled I, II, and III. Boundaries of the hydrophobic core of the membrane are represented by horizontal lines. Heavy-lined circles denote positively charged amino acid residues, whereas shaded circles indicate negatively charged residues.

accessible to proteases. Our results cannot rule out the possibility that the protein crosses the membrane only once, but they do show that a significant proportion of URF13 is protected from proteolysis, an observation more consistent with a three-membrane-spanning helical model.

Almost all membrane proteins are found in only one specific topological orientation in the membrane. Several membrane-spanning proteins have mixed orientations, but these proteins were dramatically modified through genetic manipulation of regions believed to be important determinants of membrane topology (30–32). The proposed “positive-inside” rule of von Heijne (33) suggests that the balance of positive charges on either side of a membrane-spanning domain is the primary topological determinant of prokaryotic plasma membrane proteins, the greater number of positive charges being associated with the cytoplasmic side of the membrane. Nilsson and von Heijne (30) showed that the addition or subtraction of a single positively charged residue was sufficient to determine the topology of *E. coli* leader peptidase. The model presented in Fig. 7 does not adhere in any obvious way to this rule; none of the regions of URF13 flanking the putative membrane-spanning helices has a high net positive (or negative) charge. In addition, the vector-derived segment of s10:URF13 has no net charge and apparently does not alter URF13 topology.

The membrane orientation of URF13 in *E. coli* is markedly different from that observed in mitochondria. Although we have not localized the amino terminus of URF13 in *cms-T* mitochondria, it is clear that a mixed orientation of URF13 is not found in mitochondria. These findings show that the exact mechanisms mediating URF13 insertion into the membrane differ between plant mitochondria and *E. coli*.

T toxins were the generous gift of H. W. Knoche and S. J. Danko.

Methomyl was kindly provided by E. I. duPont de Nemours and Co. Anti-SecY antiserum was the gift of W. T. Wickner (UCLA). We thank Jane Suddith for her superb technical assistance and Kim Beegle and Arlene Rice for production of MAb. This work was supported by grants from the National Science Foundation (C.S.L.) and the U.S. Department of Energy (J.N.S.) and by a fellowship from the North Carolina Biotechnology Center (K.L.K.).

1. Dewey, R. E., Timothy, D. H. & Levings, C. S., III (1987) *Proc. Natl. Acad. Sci. USA* **84**, 5374–5378.
2. Wise, R. P., Fliss, A. E., Pring, D. R. & Gengenbach, B. G. (1987) *Plant Mol. Biol.* **9**, 121–126.
3. Hack, E., Lin, C., Yang, H. & Horner, H. T. (1991) *Plant Physiol.* **95**, 861–870.
4. Dewey, R. E., Levings, C. S., III, & Timothy, D. H. (1986) *Cell* **44**, 439–449.
5. Levings, C. S., III (1990) *Science* **250**, 942–947.
6. Pring, D. R. & Lonsdale, D. M. (1989) *Annu. Rev. Phytopathol.* **27**, 483–502.
7. Dewey, R. E., Siedow, J. N., Timothy, D. H. & Levings, C. S., III (1988) *Science* **239**, 293–295.
8. Braun, C. J., Siedow, J. N., Williams, M. E. & Levings, C. S., III (1989) *Proc. Natl. Acad. Sci. USA* **86**, 4435–4439.
9. Braun, C. J., Siedow, J. N. & Levings, C. S., III (1990) *Plant Cell* **2**, 153–161.
10. Korth, K. L., Struck, F., Kaspi, C. I., Siedow, J. N. & Levings, C. S., III (1991) in *Plant Molecular Biology*, eds. Hermmann, R. G. & Larkins, B. A. (Plenum, London), pp. 375–381.
11. Sambrook, J., Fritsch, E. F. & Maniatis, T. (1989) *Molecular Cloning: A Laboratory Manual* (Cold Spring Harbor Lab., Cold Spring Harbor, NY), 2nd Ed.
12. Kunkel, T. A. (1985) *Proc. Natl. Acad. Sci. USA* **82**, 488–492.
13. Studier, F. W., Rosenberg, A. H., Dunn, J. J. & Dubendorff, J. W. (1990) *Methods Enzymol.* **185**, 60–89.
14. Harlow, E. & Lane, D. (1988) *Antibodies: A Laboratory Manual* (Cold Spring Harbor Lab., Cold Spring Harbor, NY).
15. Carter, P. B., Beegle, K. H. & Gebhard, D. H. (1986) *Vet. Clin. North Am. Small Anim. Pract.* **16**, 1171–1179.
16. Witholt, B., Boekhout, M., Brock, M., Kingma, J., van Heerikhuizen, H. & De Leij, L. (1976) *Anal. Biochem.* **74**, 160–170.
17. Smith, W. P. (1980) *J. Bacteriol.* **141**, 1142–1147.
18. Osborn, M. J. & Munson, R. (1974) *Methods Enzymol.* **31A**, 642–653.
19. Stegink, S. J. & Siedow, J. N. (1986) *Plant Physiol.* **80**, 196–201.
20. Decker, G. L. & Greenawalt, J. W. (1977) *J. Ultrastruct. Res.* **59**, 44–56.
21. Neuburger, M., Journet, E.-P., Bligny, R., Carde, J.-P. & Douce, R. (1982) *Arch. Biochem. Biophys.* **217**, 312–323.
22. Petit, P. X., Edman, K. A., Gardeström, P. & Ericson, I. (1987) *Biochim. Biophys. Acta* **890**, 377–386.
23. Reenstra, W. W., Patel, L., Rottenberg, H. & Kaback, H. R. (1980) *Biochemistry* **19**, 1–9.
24. Akiyama, Y. & Ito, K. (1987) *EMBO J.* **6**, 3465–3470.
25. Davidson, V. L., Brunden, K. R., Cramer, W. A. & Cohen, F. S. (1984) *J. Membr. Biol.* **79**, 105–118.
26. Glab, N., Wise, R. P., Pring, D. R., Jacq, C. & Slonimski, P. (1990) *Mol. Gen. Genet.* **223**, 24–32.
27. Huang, J., Lee, S.-H., Lin, C., Medici, R., Hack, E. & Myers, A. M. (1990) *EMBO J.* **9**, 339–347.
28. Eisenberg, D. (1984) *Annu. Rev. Biochem.* **53**, 595–623.
29. Nałęcz, M. J., Casey, R. P. & Azzi, A. (1986) *Methods Enzymol.* **125**, 86–108.
30. Nilsson, I. & von Heijne, G. (1990) *Cell* **62**, 1135–1141.
31. Parks, G. D., Hull, J. D. & Lamb, R. A. (1989) *J. Cell Biol.* **109**, 2023–2032.
32. Parks, G. D. & Lamb, R. A. (1991) *Cell* **64**, 777–787.
33. von Heijne, G. (1986) *EMBO J.* **5**, 3021–3027.